Vol. 48, No. 1 (2026) 54-71, DOI: 10.24874/ti.1960.06.25.09

Tribology in Industry

www.tribology.rs

RESEARCH

Synergistic Effects of Palm Methyl Ester and Cellulose Nanocrystals on Enhancing Friction and Wear Under Grease Lubrication

Zahrul Fuadi[a,*], Rudi Kurniawan[a], Ritzky Fachry[b], Ikramullah Muhammad[a], Samsul Rizal[a,c], Dieter Rahmadiawan[d,e], Shih-Chen Shi[e], Mohamad Ali Ahmad[f], Irwansyah Irwansyah[a,g]

[a]*Mechanical and Industrial Engineering Department, Universitas Syiah Kuala, Banda Aceh, Indonesia,*
[b]*Doctoral Study Program in Engineering, Faculty of Postgraduate Studies, Universitas Syiah Kuala, Universitas Syiah Kuala, Banda Aceh, Indonesia,*
[c]*Mechanical Engineering Department, Universitas Batam, Batam, Indonesia,*
[d]*Mechanical Engineering Department, Universitas Negeri Padang, Padang, Indonesia,*
[e]*Department of Mechanical Engineering, National Chen Kung University (NCKU), Tainan 70101, Taiwan,*
[f]*School of Mechanical Engineering, College of Engineering, Universiti Teknologi MARA, Malaysia,*
[g]*Mechanical Engineering Department, Universitas Teuku Umar, Meulaboh, Indonesia.*

Keywords:

Cellulose nanocrystals
Grease
Coefficient of friction
Lubricant additives

* Corresponding author:

Zahrul Fuadi
E-mail: zahrul.fuadi@usk.ac.id

Received: 18 June 2025
Revised: 7 August 2025
Accepted: 30 September2025

A B S T R A C T

This study investigates the tribological properties of eco-friendly grease lubricants formulated from palm methyl ester (PME) that incorporate cellulose nanocrystal (CNC) particles as additives. Two grease specimens were prepared: one containing CNC particles and the other without. The performance of these grease specimens was evaluated using a reciprocating pin-on-disk tribometer, with AISI 52100 steel serving as the friction material. The friction and wear characteristics of the self-mated AISI 52100 tribo-pair lubricated with the grease specimens—both with and without CNC nanoparticles—were compared to those lubricated with a commercial grease. The results show that the performance of PME grease containing CNC nanoparticles is comparable to that of commercial grease with tungsten additives. Furthermore, the tribo-pair exhibited improved friction and wear characteristics when lubricated with PME grease containing CNC nanoparticles, as opposed to being lubricated with PME grease without additives. Microscopic analysis indicates a significantly smoother and flatter surface of the contact interface when lubricated with the grease mixed with CNC particles. EDX analysis also reveals the presence of an aluminum oxide layer at the contact interface of the tribo-pair when lubricated with PME grease containing CNC particles, appears to be responsible for protecting the contact area from severe friction and wear.

1. INTRODUCTION

The accelerating pace of industrial transformation, driven by the Fourth Industrial Revolution and initiatives such as the ASEAN Economic Community, has significantly intensified the demand for innovative, competitive, and sustainable technological solutions [1]. In this context, sectors such as manufacturing and mechanical engineering are under increasing pressure to enhance performance, minimize energy losses, and extend the lifespan of components by improving friction and wear control. Consequently, tribology — the science of friction, wear, and lubrication — plays a pivotal role in promoting industrial efficiency and competitiveness [2].

Simultaneously, increasing global concerns about environmental sustainability have sparked a growing interest in renewable and eco-friendly lubricants. One promising strategy to enhance the biodegradability of these lubricants is the use of base oils and additives derived from natural, renewable resources [3]. Lubricants can be categorized into several groups: liquid lubricants, semi-solid lubricants (such as grease), solid lubricants, and gas lubricants. Among these, liquid lubricants and grease are the most commonly used types in industry. Nowadays, research and development in the field of lubrication is increasingly focusing on renewable and environmentally friendly lubricant materials derived from sustainable sources, both as base materials and additives [4,5]. Numerous studies have shown that vegetable oil-based lubricants exhibit tribological properties comparable to those of mineral oil-based lubricants [6,7].

Various additives derived from natural ingredients have been utilized to enhance the performance of vegetable oil-based lubricants. One such natural nanoparticle additive that has demonstrated effectiveness in improving renewable oil-based lubricants is nanocellulose [8]. Cellulose, a vital biopolymer found in nature, is a renewable, non-toxic, biodegradable, and biocompatible material [9-13]. This substance can serve as an environmentally friendly lubricant additive, reducing friction and increasing wear resistance [14,15]. A specific type of cellulose that has been employed as an additive is Crystalline Nanocellulose (CNC). This product is crystalline in nature and can be produced through hydrolysis, which removes amorphous and semi-crystalline regions from cellulose fibrils [16]. CNCs typically exhibit a rod-like morphology, with diameters ranging from 5 to 50 nm and lengths between 100 and 1000 nm. Due to its hard and diminutive crystalline properties, nanocellulose can effectively fit into the gaps of interacting surfaces, thereby protecting them from excessive wear.

Recent studies have demonstrated that CNC particles offer excellent tribological benefits when dispersed in lubricant oils. For instance, Awang et al. [17] reported significant reductions in the coefficient of friction (COF) and wear rate when CNC nanoparticles were added to base oil and tested using a piston–skirt liner tribometer. The optimal performance was observed with a 0.1 wt% concentration of CNC under both high-speed/low-load (500 rpm, 39.24 N) and low-speed/high-load (200 rpm, 98.1 N) conditions.

At this concentration, the wear rate was reduced by up to 69%, and the COF values were consistently lower than those of base oil SAE 40. SEM analysis of worn surfaces revealed that CNC-containing oils produced smoother and flatter surfaces with fewer grooves and debris. In contrast, the base oil without CNC showed extensive exfoliation and wear marks. EDX results further confirmed the presence of carbon and aluminum elements, suggesting surface layer exfoliation during friction.

One of the primary weaknesses of nanocellulose materials as lubricant additives is the aggregation of nanoparticles within the base oil. This phenomenon is attributed to the high surface energy of the nanoparticles and their density, which ranges from 1.582 to 1.599 g/cm^3—significantly greater than that of vegetable oil, which has a density of 0.85 to 0.95 g/cm^3 [18,19]. As a result, the stability of the lubricant is compromised, hindering the nanoparticles' ability to effectively penetrate the contact gaps of friction surfaces to reduce friction. This instability may even lead to abrasive wear [20]. Although the incorporation of a surface modifier can enhance the oil's viscosity, transforming it into a semi-solid oleogel, the stability of the resulting dispersion remains limited [21].

The advantages of cellulose particles as additives can be optimized when they are incorporated into semi-solid lubricants or greases. Grease typically consists of a semi-solid structure composed of 65-95% base oil, 3-30% thickener, and 0-10% additives. Extensive research has been conducted on grease formulations based on plant oils, including castor oil [22], neem oil [23], corn oil, olive oil, and coconut oil [24], and other various plants' oils [25,26]. Additionally, various nano-sized additives have been utilized in grease lubricants, such as zinc oxide (ZnO) and silicon dioxide (SiO_2) [27,28], silica and silicon carbide [29], and nano-sized boron nitride (BN) combined with molybdenum disulfide (MoS_2) [30].

It has also been reported that palm methyl ester and nanocellulose particles are renewable materials with the potential to function as lubricants due to their excellent wear protection properties [21]. However, a significant challenge associated with palm methyl ester lubricants containing nanocellulose additives in liquid form is the instability of the dispersion of cellulose particles within the ester. This instability results in the formation of agglomerates, which ultimately diminishes the lubrication effectiveness. Conversely, due to its characteristics, a palm methyl ester-based lubricant with nanocellulose particles as an additive may be more effective in a form of semi-solid or grease, where the agglomerates formed could provide additional benefits.

Several studies on environmentally friendly grease lubricants incorporating cellulose particle additives have been published, including those made from triethyl citrate mixed with micro fibrillated cellulose [31]. However, there is still limited research on grease lubricants that utilize palm methyl ester as a base ingredient along with cellulose particle additives.

This study investigates the performance of lubrication, specifically focusing on the friction and wear of metallic tribo-pair materials lubricated with grease containing palm methyl ester as a base ingredient, along with CNC particles as additive. The objective of this study is to evaluate the role of cellulose particles in minimizing surface wear on the friction surfaces of metal materials when incorporated as additive in PME based grease. It is anticipated that this evaluation will enhance the understanding of the effectiveness of PME-based grease lubricants and cellulose particle additives as environmentally friendly lubricants.

2. MATERIALS AND METHODS

This study consists of several steps, i.e., preparation of CNC, preparation of grease specimens, friction testing using a tribometer, wear evaluation, and surface characterization. Each step is explained as follows:

2.1 CNC preparation

Cellulose nanocrystal particles were produced from the grass plant known as Pennisetum purpureum. Initially, the grass stems were collected and allowed to dry. The stems were then cut into smaller pieces and treated with sodium hydroxide to remove hemicellulose, lignin, and surface impurities. The resulting fiber was rinsed with water until it reached a neutral pH level and then dried in an oven. After drying, the fiber was chopped and soaked in sodium hypochlorite (NaOCl) for 24 hours. The bleached fiber was subsequently washed until it reached a neutral pH and allowed to dry. The process continued with acid hydrolysis using sulfuric acid (H2SO4) for one hour, followed by silane treatment, which involved soaking and heating the fiber at 50°C for two hours with a mixture of 3-aminopropyltriethoxysilane and methanol in a 9:1 ratio. The mixture was then centrifuged until it reached a neutral pH level. The obtained suspension was sonicated and freeze-dried to produce the CNC product. A detailed explanation of CNC preparation has been reported previously [32].

The dried CNC product was mixed with ethanol to create a suspension that was subsequently used to prepare the grease specimens.

2.2 Grease specimens

In this study, we have produced several viscous compounds to use as grease specimens. Our objective was to create compounds with high viscosity to prevent cellulose particles from settling during testing. To achieve biodegradability of these compound, Palm Methyl Ester (PME) was utilized as the base oil. PME is derived from the transesterification of crude palm oil and has been

employed as a fuel substitute for diesel engines, either in its pure form or as a mixture with petroleum diesel. The PME used in this study primarily consists of methyl palmitate, oleic acid, and stearic acid [33]. Palm methyl ester also contains residual oxygenated compounds, such as unreacted glycerol and trace esters, as byproducts of the transesterification process.

(a) (b) (c)

Fig. 1. Grease specimens used in this study: Palm Methyl Ester (PME) grease (a), Palm Methyl Ester with Cellulose (PME-C) grease (b), and Petroleum (Petro) grease (c).

Two grease specimens were prepared for this study: PME-based without CNC particles (Fig. 1(a)) and PME-based with CNC particles (Fig. 1(b)). The PME-based without CNC particles is referred to as PME grease, while the one with CNC particles is called PME-C grease. To facilitate a comparison of friction and wear properties, a petroleum-based grease was also utilized (Fig. 1(c)), referred to as Petro grease. This petroleum grease was commercially obtained and is marketed as lithium-based grease.

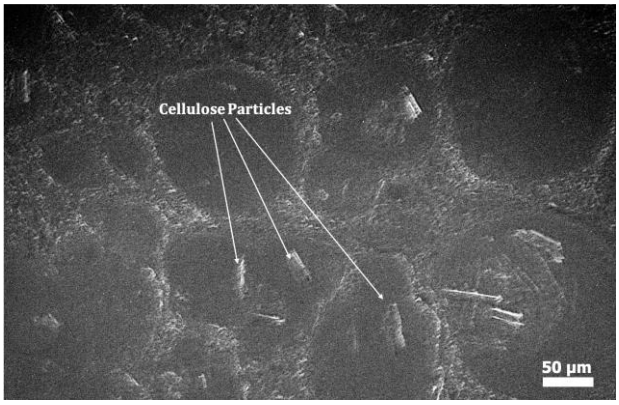

Fig. 2. Optical microscopic image of grease specimens shown in Fig. 1(b) indicating the presence of cellulose particles.

The PME grease and PME-C grease specimens were each prepared using 100 ml of palm methyl ester. To achieve a high viscosity compound, sodium hydroxide was employed to induce a saponification reaction with the free fatty acids in the palm methyl ester, producing sodium soaps that function as thickeners in the grease formulation. During the preparation process, the PME fluid was placed in a glass beaker and heated. Once the temperature reached 75°C, 5 ml of NaOH solution was added, and the mixture was stirred while being allowed to cool. For the PME-C grease specimen, in addition to the 5 ml of NaOH solution, an additional 10 ml of a suspension containing ethanol and 1 mg of cellulose nanocrystals was incorporated. The cellulose particles in the PME-C grease are illustrated in Fig. 2. The size of the cellulose particles ranges from 10 to 50 nm in length and 5 to 10 nm in circumference.

2.3 Elemental analysis by spectroil

Elemental analysis was performed using the Spectroil Q100, an atomic emission spectrometer, as shown in Fig. 3, to detect the elements present in the specified commercial reference greases. The test conforms to ASTM D6595, allowing the detection of a total of 33 metal and non-metal elements in the parts per million (ppm) range. In practice, a grease sample was applied to the lens surface and then burned in the spectrometer. The test was repeated five times for each sample to ensure result accuracy.

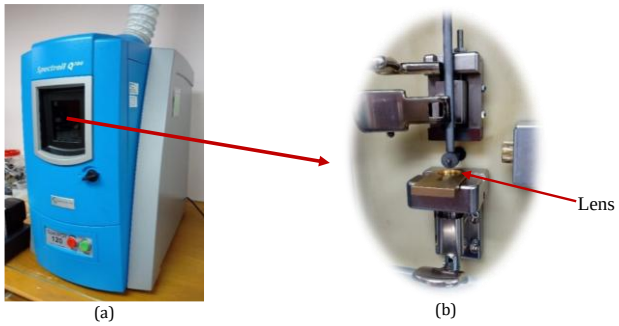

(a) (b)

Fig. 3. Spectroil Q100 spectrometer (a), and test specimen inside the spectrometer (b).

2.4 Friction and wear evaluation

To evaluate the lubrication performance of the grease, a reciprocating pin-on-disk tribometer was utilized. The tribometer comprises a cantilever beam and a shallow disk chamber. The chamber is mounted on a base and is moved in a reciprocating motion by an electric motor, a swash bearing, and a linear guide (see Fig. 4(a)). The pin is affixed to the cantilever beam, where the normal force is applied through gravitational load. A pair of strain gauges is installed on the cantilever beam to serve as the load sensor (see Fig. 4(b)).

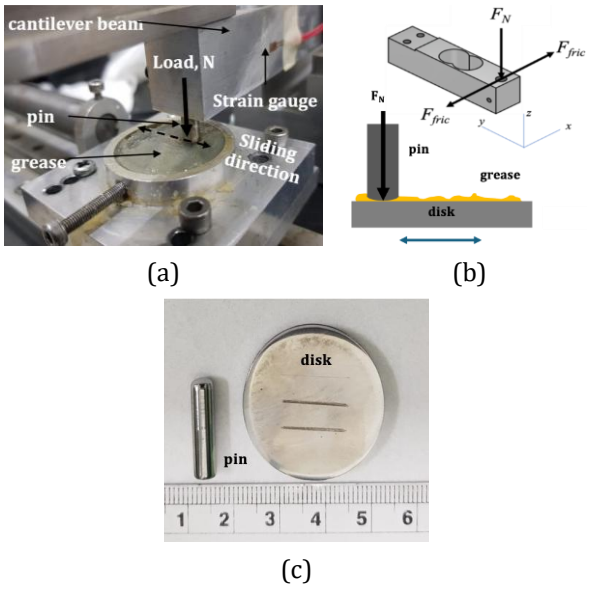

Fig. 4. Friction test configuration of pin-on-disk for friction and wear evaluation in this study: reciprocating sliding direction of pin-on-disk with grease on the contact interface (a), schematic diagram of cantilever beam and pin-on-disk configuration (b), pin and disk (c).

The pin and disc are made of stainless steel designated as AISI 52100 (see Fig. 4(c)). The disc specimen has a diameter of 30 mm and a thickness of 5 mm, and it was manufactured from a 30 mm cylindrical bar. In contrast, the pin specimen was directly taken from a bearing and has a length of 20 mm and a diameter of 4 mm. The contact interfaces of both the pin and disc specimens were polished to achieve a relatively smooth surface finish. The surfaces were progressively rubbed with emery paper up to grit #7000 and finished with 1 μm diamond paste. The tip of the pin is hemispherical, featuring a contact radius of 10 mm.

To simulate friction under both low and severe contact conditions, friction tests were conducted with normal forces of 6 N and 12 N. The contact configuration consisted of a hemispherical surface (10 mm radius) in contact with a flat plane. The initial contact pressures (Hertzian) for the respective normal forces were 0.825 GPa and 1.039 GPa, given a material Young's modulus (E) of 200 GPa and a Poisson's ratio of 0.3. Prior to the commencement of each friction test, a layer of grease approximately 2 mm thick was applied to the disc surface (see Fig. 4(b)). The friction test was conducted for a duration of two hours, during which no additional grease was applied.

The friction tests were conducted at room temperature, specifically at 26°C and relative humidity of 75%. During the friction tests, the disc was moved in a reciprocating motion. Each reciprocating cycle was completed in 3 seconds, covering a sliding distance of 30 mm. The maximum sliding speed reached 0.2 m/s. A data acquisition module based on the Kyowa System was utilized to collect the friction data at a sampling frequency of 10 Hz. The cantilever beam load sensor was calibrated for the normal load using gravitational forces.

The friction tests were conducted for two hours, covering a total sliding distance of 72 meters. The wear evaluation focused on the pin's worn surface, as it is continuously in sliding contact during the friction process. The morphology and composition of the worn contact interface were characterized using scanning electron microscopy (SEM) and energy-dispersive X-ray spectroscopy (EDX) to gain insights into the wear mechanisms.

2.5 Grease extreme pressure (EP) by Four ball tester – ASTM D2596

EP test was carried out according to ASTM D2596, with the purpose to determine the load-carrying capacity of the greases and the relative ability to prevent wear under high-pressure conditions. Similar sample preparation procedure as in WP, yet only 10 seconds was taken for each test, with 1760 rpm speed at 30°C. Started from 24 kg, the load was increased stepwise in every run with a new set of balls until the test balls are welded together or seizure. The final seizure load where the load of the four balls become welded to each other indicates the ability of the grease to withstand pressure and maintain a protective film between moving surfaces. The test conditions is given in Table 1.

Table 1. Extreme Pressure Test Conditions.

Speed (rpm)	Load (kg)	Duration	Temp. (°C)	Remarks
1760 ± 40	At increasing load until weld occurs	Series of 10 seconds	27 ± 8	Force applied through torque wrench on ball pot nut approx. 50±5 lb-ft for optimum test repeatability.

3. RESULTS AND DISCUSSIONS

3.1 Grease elemental contents

The elemental analysis had been carried out with the purpose of identifying the elements present in the two grease specimens using Spectroil Q100. Table 2 portrayed the selected elements contained in the identified greases representing the thickener and additive types.

Table 2. Grease Elements in ppm.

Palm Methyl Ester (PME) in ppm	Palm Methyl Ester with Cellulose (PME-C) in ppm
Ca – 3.5	-
Ce – 7.5	Ce – 6.2
K – 13.3	K – 5.6
Na – 4096.7	Na – 1861.4

The elemental analysis indicates that the grease contains significant elements. PME-C grease exhibits fewer elements due to the chemical reactions that occur during the processing. PME grease, which contains calcium, has the ability to thicken while also providing water resistance and thermal stability.

3.2 Friction coefficient

Figure 5 and Figure 6 illustrate the normalized coefficients of friction for normal loads of 6 N and 12 N, respectively. In these figures, the friction coefficient values represent the friction experienced over a duration of 7200 seconds, corresponding to a sliding distance of 72 meters.

Figure 5 indicates that at a normal load of 6 N, corresponding to an initial contact pressure of 0.825 GPa, the friction pairs exhibit relatively similar coefficients of friction at the beginning of sliding, which is 0.1. However, as sliding progresses, Petro grease specimen demonstrates superior performance, as evidenced by a friction coefficient value of less than 0.1. In contrast, PME grease specimen shows a gradual increase in the coefficient of friction by the end of the sliding test. PME-C grease specimen exhibits the highest coefficient of friction among the three specimens, although this value remains stable at 0.12 for the majority of the sliding test period.

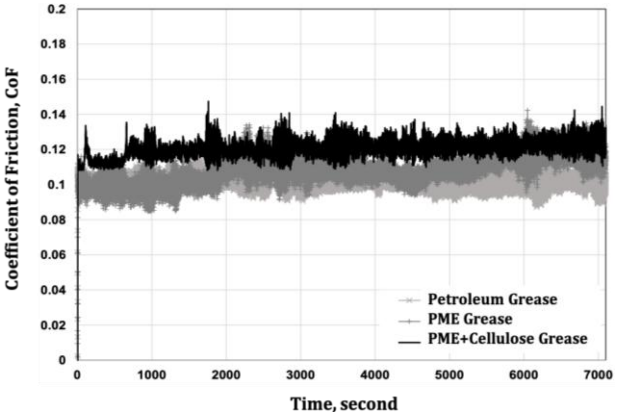

Fig. 5. COF comparison among grease specimens at a normal load of 6 N.

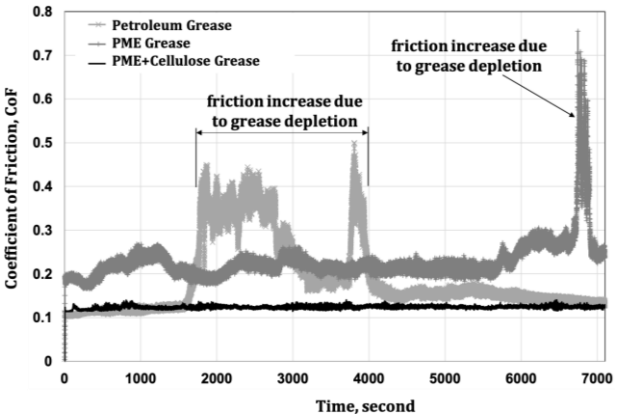

Fig. 6. COF comparison among grease specimens at a normal load of 12 N.

The superior properties of the Petro grease specimen are further illustrated in Figure 6. The coefficient of friction for the grease specimens remains constant at 0.1, even as the normal load increases to 12 N, corresponding to an initial contact pressure of 1.039 GPa. This coefficient of friction remains stable for approximately 1,600 seconds of sliding time, which corresponds to a sliding distance of 16 meters. Following this period, the coefficient of friction exhibits erratic and unstable behavior, reaching nearly 0.5 before stabilizing again around 4,000 seconds of sliding time. The value gradually decreases back to 0.1 by the end of the test. The unstable behavior of friction in this case is attributed to the drying of the grease at the contact interface. As sliding continues, it appears that some grease is drawn back to the contact interface through the sliding process, providing lubrication once again and reducing the coefficient of friction back to 0.1 by the conclusion of the sliding test.

In the case of the PME grease specimen, the coefficient of friction began at a value of 0.2 at the onset of sliding and fluctuated to approximately 0.3 for the majority of the sliding test. Near the end of the sliding test, the friction spiked to a significantly high value of around 0.7. This spike in the friction coefficient appears to have been caused by the depletion of grease at the contact interface. Similar to what occurred with the Petro grease specimen, some grease re-entered the contact interface, resulting in a decrease in friction back to the value observed before the spike.

The PME-C grease specimen, in contrast, performs significantly better than the other two specimens under a higher normal force. The coefficient of friction began at approximately 0.13 and remained constant throughout the sliding process. Grease depletion at the contact interface did not occur during the sliding test. This is presumably due to the cellulose particles retaining some PME fluid, preventing it from solidifying due to the sodium hydroxide. During the sliding test, it was observed that the contact interface with PME-C grease lubrication appeared wetter than in the other two cases.

Grease depletion was not observed at low contact pressures (a normal load of 6 N). It appears that grease depletion occurs due to locally high temperatures under high contact pressure. In the case of PME-C grease, the cellulose particles seem to bind more oil, resulting in a wetter grease. This allows some of the PME oil that remains free to flow into the sliding track. Consequently, the sliding track does not dry during the sliding test when lubricated with PME-C grease.

Grease depletion on the sliding track can lead to increased friction in most cases; however, the presence of moisture on the sliding track in the case of PME-C grease may not necessarily account for the observed low friction under these conditions. As illustrated in Figure 6, the coefficient of friction for Petro grease is lower than that of PME grease during the first 1600 seconds of sliding. Within this timeframe, the coefficient of friction for PME-C grease is relatively similar to that of Petro grease, while PME grease alone exhibits a higher coefficient of friction. This indicates that PME grease alone is insufficient for reducing friction under high normal loads. Consequently, the occurrence of low and stable friction with PME-C grease lubrication cannot be attributed to the sliding track being moist, as some of the PME oil may bind to cellulose particles during the friction process.

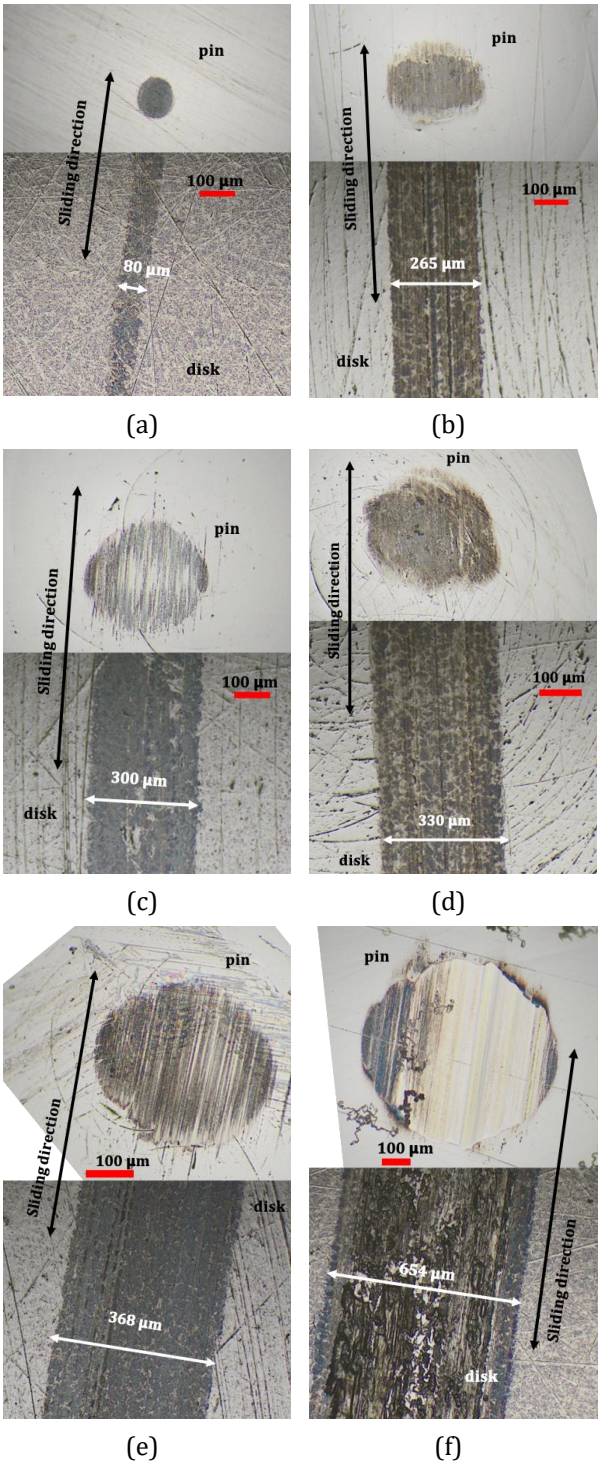

Fig. 7. Width of wear tracks at various normal loads and grease specimens; Petro grease at normal load of 6 N (a), PME-C grease at normal load of 6 N (b), PME grease at normal load of 6 N (c), PME-C grease at normal load of 12 N (d), PME grease at normal load of 12 N (e), and Petro grease at normal load of 12 N (f).

Therefore, an alternative explanation is needed to account for the low friction observed under PME-C and Petro grease conditions.

3.3 Specific wear rate

Figure 7 illustrates the images of sliding tracks subjected to various lubricants and normal loads. At a normal load of 6 N, the Petro grease specimen exhibits a significantly smaller wear scar on the pin, with a diameter of 80 μm (see Fig. 7(a)). This worn scar corresponds to a specific wear rate of approximately 6.18 x 10^{-9} mm^3/N·m. In contrast, the wear scar diameters for the other two grease specimens are considerably larger than that of the Petro grease specimen. The PME-C grease shows a diameter of 265 mm (see Fig. 7(b)), which corresponds to a specific wear rate of 7.45 x 10^{-9} mm^3/N·m. Meanwhile, for the PME grease, the diameter measures 300 mm (see Fig. 7(c)), resulting in a specific wear rate of 1.54 x 10^{-9} mm^3/N·m.

At a normal load of 12 N, the wear scar on the pin can be observed in Fig. 7(d)-(f) for the PME-C grease, PME grease, and Petro grease specimens, respectively. The figures indicate that the Petro grease specimen exhibits the largest wear scar diameter at 654 μm, followed by the PME grease specimen at 368 μm. The PME-C grease shows the smallest wear scar diameter on the pin, measuring 330 μm. However, in this context, comparing the width of the wear scar or the specific wear rate is not relevant. This is because the large wear scar diameters observed in the Petro grease and PME grease specimens are associated with unstable friction, during which the sliding interface experienced periods of grease depletion from the contact area, as indicated by the high friction coefficient (see Fig. 6). Whereas small wear scar diameter in the case of PME-C grease specimens is associated with stable friction across the entire friction test.

Nevertheless, the surface profiles of the Petro grease specimen (see Fig. 8(a-b)) and the PME grease specimen (see Fig. 8(c-d)) exhibit significantly greater roughness compared to the surface of the PME-C grease specimen (see Fig. 7(e-f)). The friction surfaces of the Petro grease and PME grease specimens have an area surface roughness, Sa, of 1.982 μm and 0.932 μm, respectively. In contrast, the area surface roughness of the worn scar area in the PME-C grease specimen measures only 0.439 μm. A relatively smoother contact interface can also be observed on the sliding tracks of the disc counterparts (see Fig. 7(d) for PME-C grease, Fig. Fig. 7(e) for PME grease, and 7(f) for Petro grease).

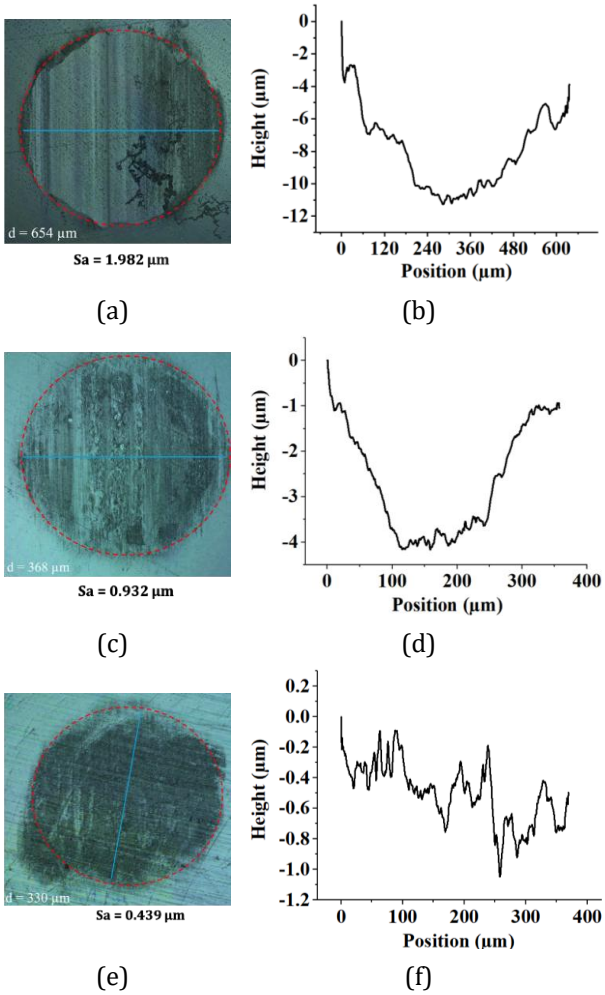

Fig. 8. Width of wear track and area surface roughness (Sa) for various grease specimens at normal load of 12 N; Petro grease (a-b), PME grease (c-d), and PME-C grease (e-f).

It appears that cellulose particles in the grease play a crucial role in protecting the contact interface during severe friction under relatively high contact pressure. As previously reported, cellulose particles have been shown to be effective in reducing friction and wear at the contact interface [21,34-36]. Microfibrils reduce friction and wear of the contact pair by filling surface irregularities and forming a protective tribofilm on the contact interface [31].

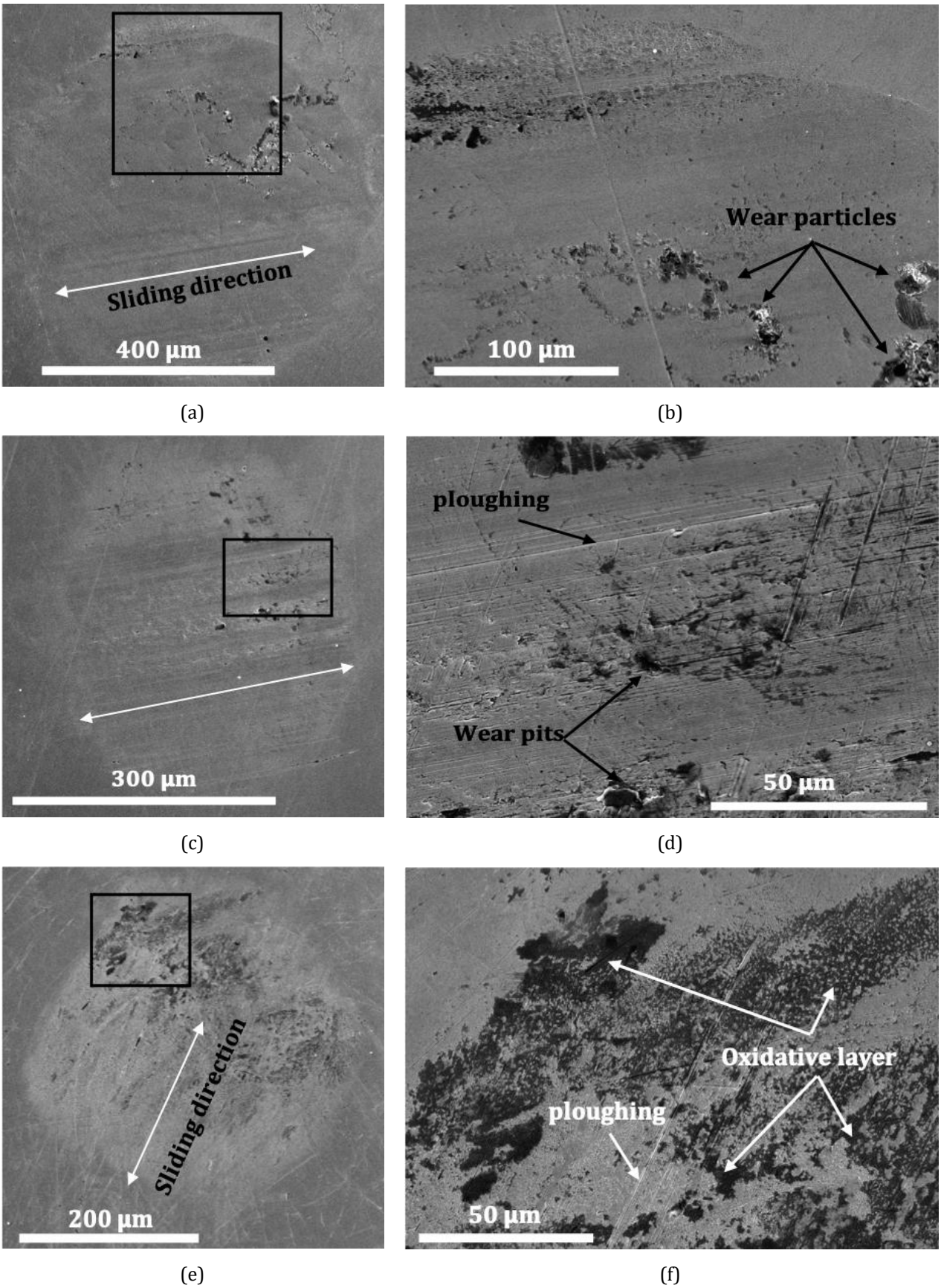

Fig. 9. Microscopic images of the worn scars on the pins' contact interface under a normal load of 12 N, using Petro grease (a-b), PME grease (c-d), and PME-C grease (e-f).

3.4 Wear mechanism

To further understand the role of cellulose particles in reducing friction and wear on the tribo-pair, a detailed observation of the contact interface was conducted. The analysis focused on the contact interface under a normal load of 12 N, as there is a greater likelihood of tribofilm formation at elevated contact loads.

At a normal load of 12 N, the worn area of the pin lubricated with Petro grease, despite exhibiting relatively high wear, appears to be relatively free from surface pits (see Fig. 9(a-b)). In this instance, surface wear seems to occur in an abrasive manner. Although the contact interface experienced grease depletion during the sliding process, leading to increased friction, this condition did not result in significant material removal from the contact pair, as the surface remains relatively free from grooves. This phenomenon may be attributed to additives in the Petro grease that function as nano-sized abrasive materials, enabling the friction surface to experience uniform wear despite high friction levels. Such surface conditions can lead to a reduction in friction when the lubricant re-enters the contact area. This explains why the friction coefficient returns to a low value after the grease re-enters the friction surface (see Fig. 6 for the Petro grease condition).

On the contrary, noticeably large surface pits occur on the contact interface under PME grease conditions (see Fig. 9(c-d)). Wear grooves are also present on the contact interface, indicating the occurrence of heavy ploughing (see also Fig. 7(c) and Fig. 7(e)). The surface pits appear to be the result of friction spikes during grease depletion, as indicated by the friction curve in Fig. 6 for the PME grease specimen. Although the friction returns to a lower value as the grease re-enters the contact interface, the already damaged surface could cause high friction again if the friction test continues for an extended period.

A relatively smooth contact interface is observed in the case of PME-C grease conditions (see Fig. 9(e-f)), despite the relatively high contact pressure. No noticeable surface pits are present on the contact interface; however, some ploughing grooves do occur. The most prominent surface feature is the presence of a tribo-layer on the contact interface, particularly at the edge of the sliding track, as illustrated in Fig. 9(f). This layer appears to be an oxidative film formed during the sliding process. The oxidative layer was not observed in cases of friction under Petro grease and PME grease conditions. Therefore, its formation indicates the involvement of cellulose particles, which occur at relatively high contact pressures during friction due to a tribo-chemical process. It seems that this layer is responsible for the low friction and wear observed under PME-C grease conditions.

A detailed analysis of the contact interface reveals that the tribofilm formed under PME-C grease consists of oxygen and aluminum (see Fig. 10(c),(d)), in addition to the elements that constitute the bulk material of AISI 52100, which includes iron, chromium, manganese, carbon, and silicon. Notably, aluminum was detected at the contact interface, where a blackish surface layer is present. Therefore, this black surface layer appears to be an oxidative layer composed of oxygen and aluminum. However, the source of aluminum at the contact interface in this specific case remains unclear, as aluminum is not listed among the elements of AISI 52100 carbon steel, nor was it included in the cellulose production process.

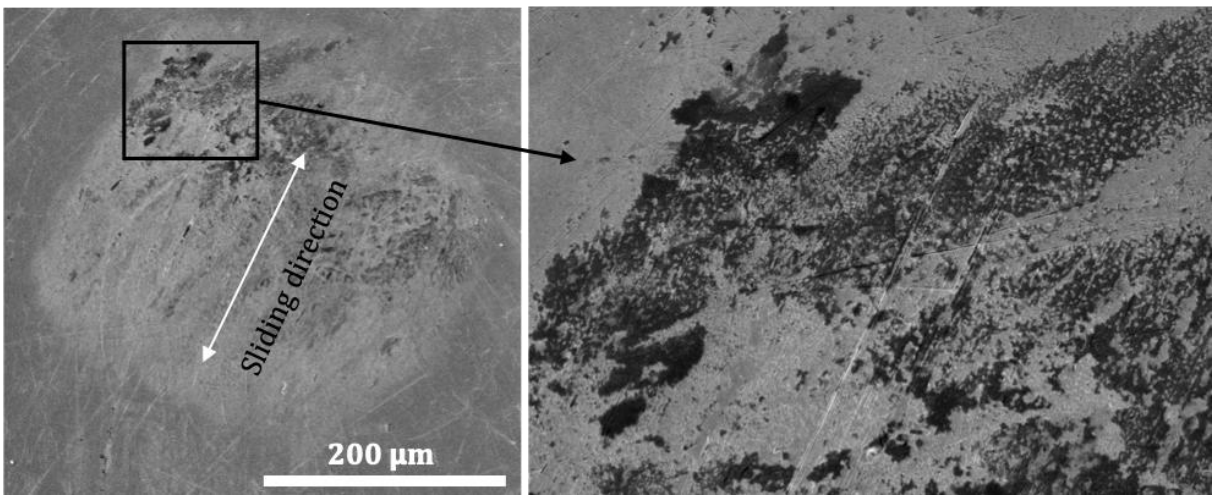

(a)

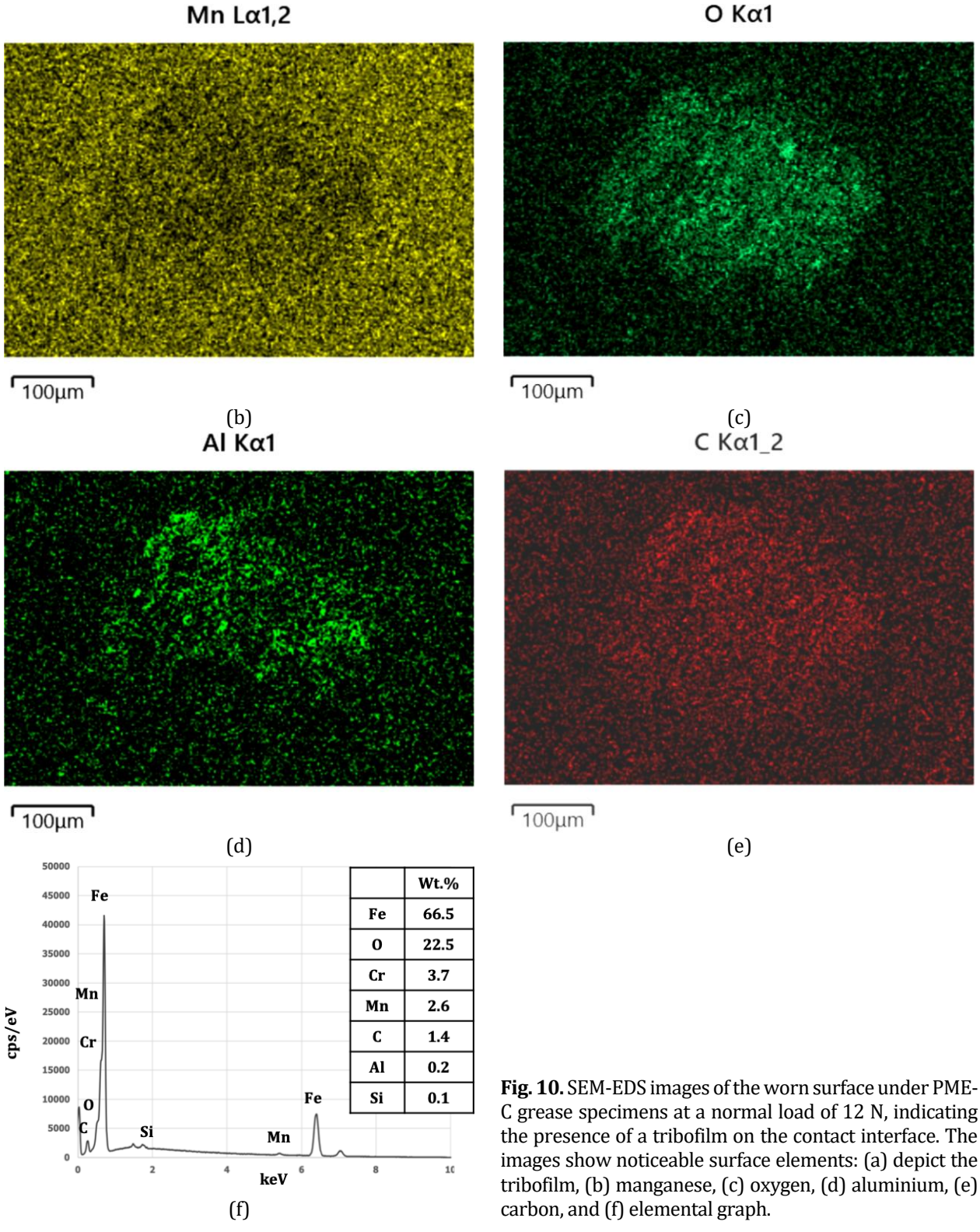

Fig. 10. SEM-EDS images of the worn surface under PME-C grease specimens at a normal load of 12 N, indicating the presence of a tribofilm on the contact interface. The images show noticeable surface elements: (a) depict the tribofilm, (b) manganese, (c) oxygen, (d) aluminium, (e) carbon, and (f) elemental graph.

In the case of Petro grease, wear particles (debris) can be detected at the contact interface (see Fig. 11(a), as well as Fig. 9(b)). Oxygen elements are present at the locations where the debris is found, both on the sliding contact and outside of it (see Fig. 11(c)), along with carbon elements (see Fig. 11(e)). It can also be observed that the area where the debris is found lacks manganese (see Fig. 11(b)), confirming that the particles are worn debris covering the contact interface. Additionally, tungsten is detected in this case (see Fig. 11(f)), indicating that the Petro grease specimen contains tungsten, likely as an additive. Tungsten (W) has been shown as one of the most effective nano-additives in lubricants [37-39]. Tungsten is an exceptionally hard material that can be engineered at the nanoscale to enhance

the load-carrying capacity of lubricants, thereby improving their effectiveness in reducing friction and wear. Here, the relatively clean and groove-free contact interface observed under the Petro grease condition can be attributed to the presence of tungsten particles, likely at the nanoscale. The additive seems to effectively restore the friction coefficient to a low level, as indicated by the friction curve in Fig. 6. Notably, aluminum was not detected in the contact interface (see Fig. 11(d) and (f)).

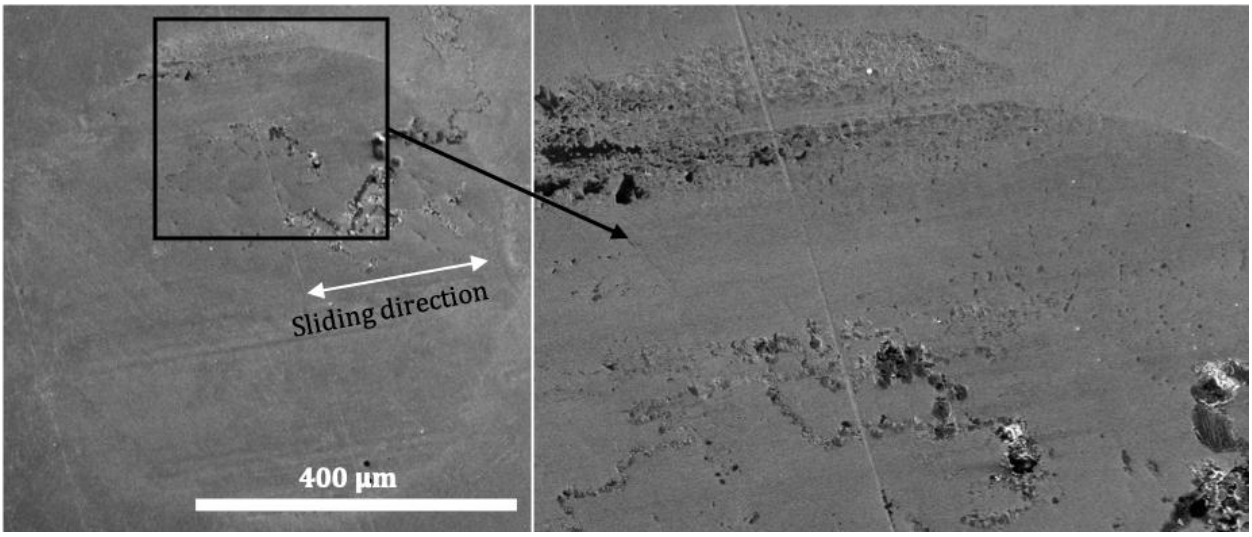

(a)

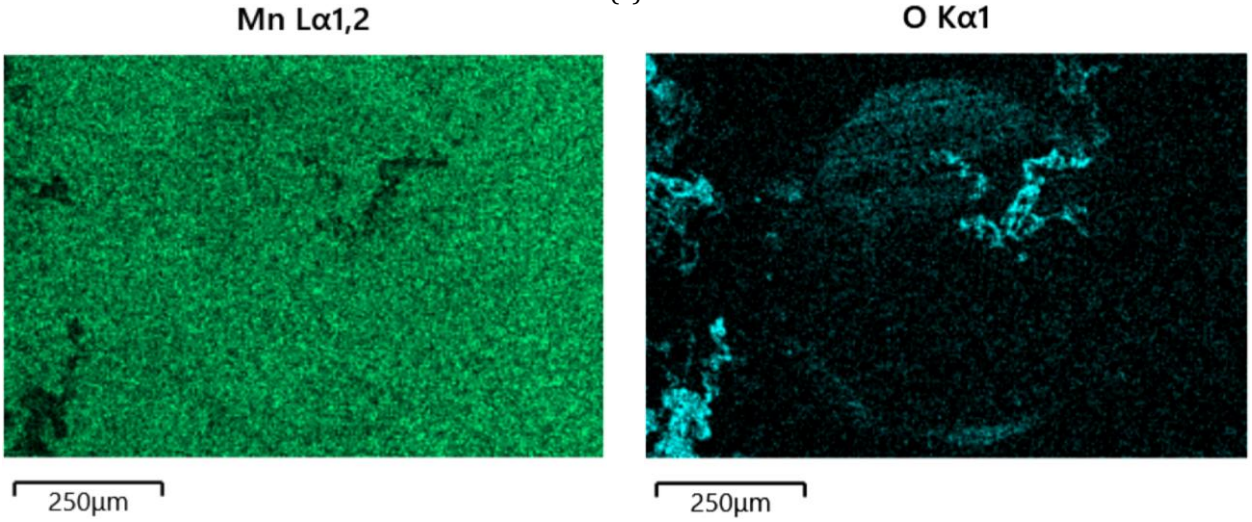

(b) (c)

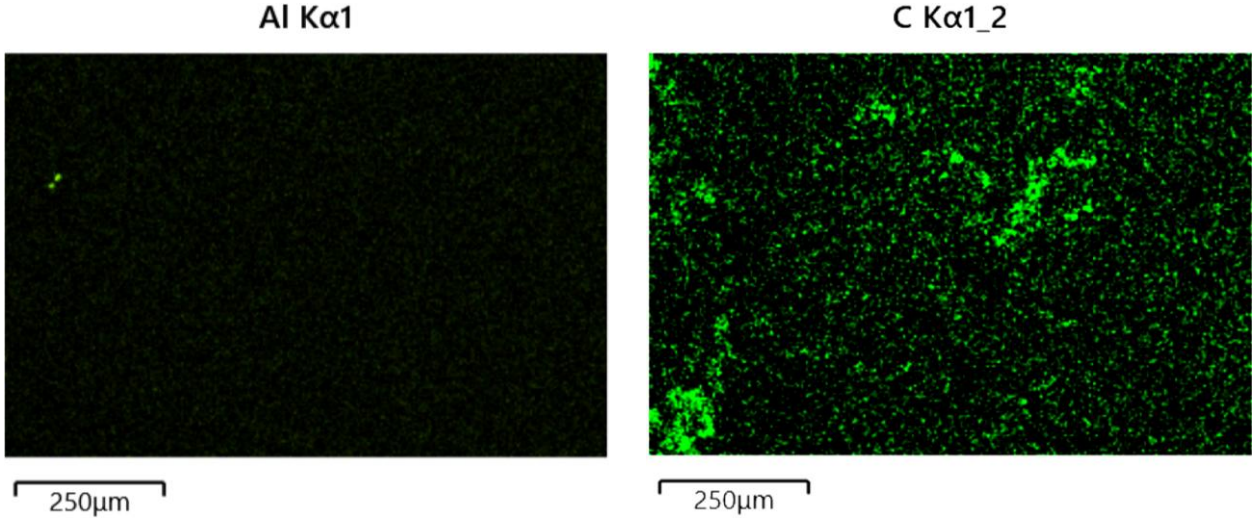

(d) (e)

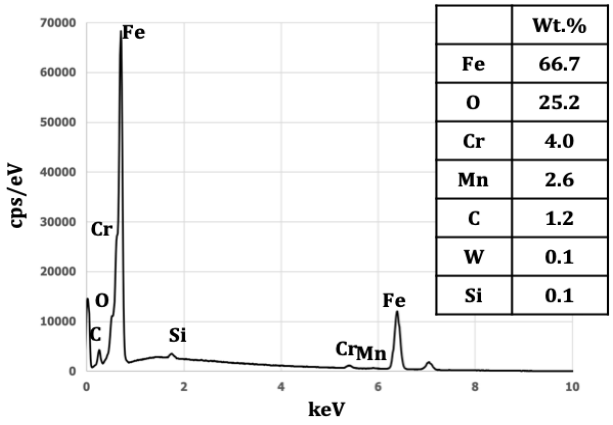

	Wt.%
Fe	66.7
O	25.2
Cr	4.0
Mn	2.6
C	1.2
W	0.1
Si	0.1

(f)

Fig. 11. SEM-EDS images of the worn surface under Petro grease specimens at a normal load of 12 N. The images of worn scar area display some wear debris (a) comprised of oxygen (c) and carbon (e). No significant manganese (b) and aluminium (d) were identified, while tungsten (additive material) was detected on the contact interface (f).

The tribofilm observed in the PME grease specimen primarily consists of an oxygen layer (see Fig. 12(e)). The presence of carbon and manganese elements at the contact interface is minimal, similar to the observations made with Petro grease and PME-C grease specimens. Therefore, it is likely that the tribofilm layer formed under PME grease lubrication is composed of a metal oxide, most probably manganese oxide, due to the high reactivity of manganese. Aluminum, on the other hand, is detected locally, particularly in areas where pits are present. In this context, it appears that aluminum contributes negligibly to friction and wear.

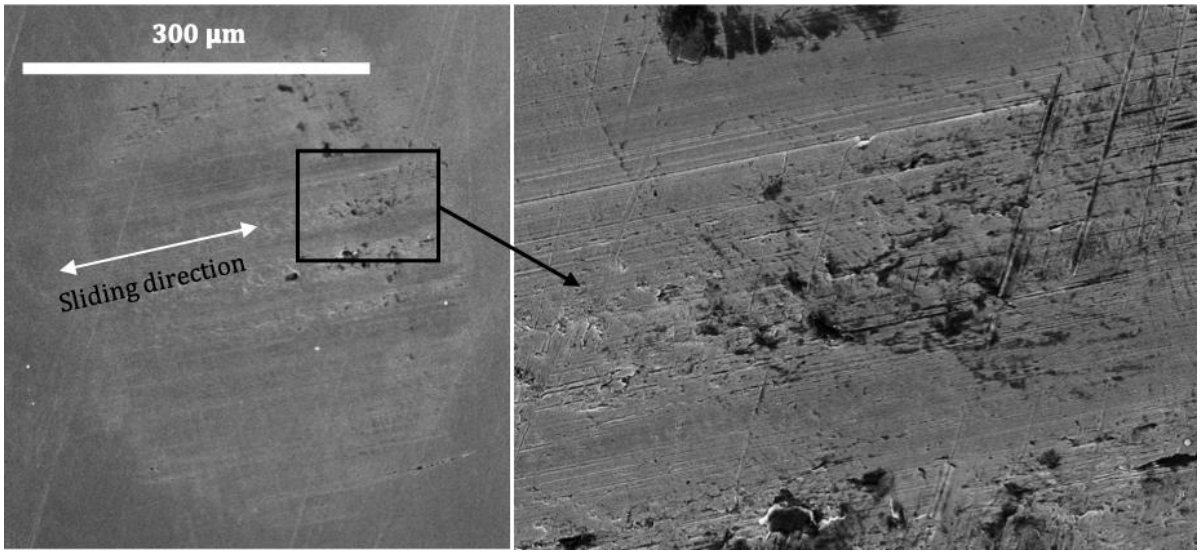

(a)

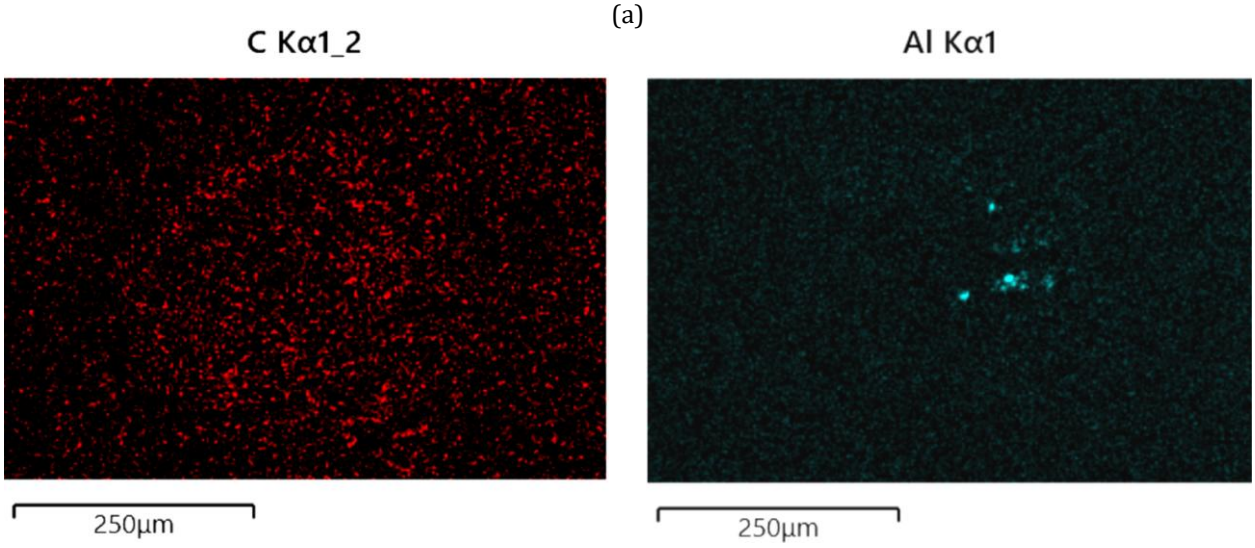

(b) (c)

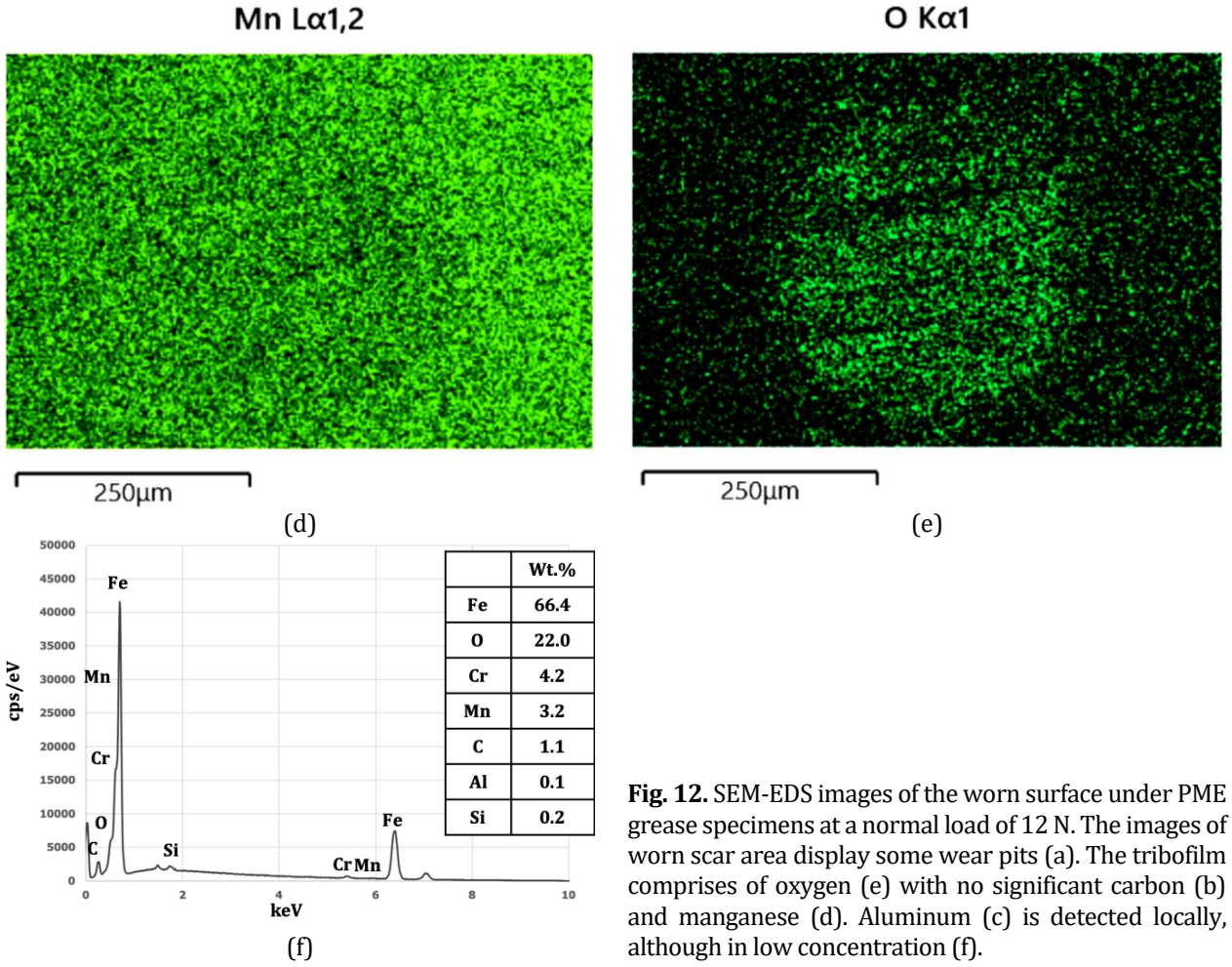

Fig. 12. SEM-EDS images of the worn surface under PME grease specimens at a normal load of 12 N. The images of worn scar area display some wear pits (a). The tribofilm comprises of oxygen (e) with no significant carbon (b) and manganese (d). Aluminum (c) is detected locally, although in low concentration (f).

Based on the results, it can be concluded that cellulose particles are highly effective in reducing friction and wear, particularly under conditions of high contact pressure. The performance of cellulose particles in this context is comparable to that of tungsten particles used in commercial grease lubricants. This similarity is evident from the comparable coefficients of friction observed under the lubrication conditions of Petro grease and PME-C grease.

It has been reported that cellulose particles used as additives in liquid lubricant formulations can reduce friction by forming a thin tribo-layer on steel-to-steel contact surfaces, thereby protecting the surfaces from friction and wear [40]. Another research indicates that CNC particles can fill the pits and grooves on the rubbing surface, providing a polishing effect that allows the contact surface to remain relatively free from scratches [17]. This mending effect can also lead to the formation of a boundary film layer, which further reduces friction. The crystalline structure of cellulose particles, particularly in the form of nanofibrils, can fill the gaps of surface irregularities at low concentrations, while at higher concentrations, it can form a tribofilm layer that minimizes friction and wear [31]. In this study, surface characterization was conducted to determine whether a crystalline layer exists at the contact interface. However, such a layer was not found, presumably due to the low concentration of cellulose. Consequently, the cellulose particles were sufficient to fill surface gaps but inadequate to produce a boundary layer with a crystalline structure.

Previous research utilizing petrodiesel fuel and low carbon steel as the tribo-pair [41] revealed that the manganese content in the material was reactive that lead to rapid surface roughening. This condition improved when Palm Methyl Ester (PME) was used as the lubricant, as the oxygen content in the lubricant reacts directly with and binds the loose manganese, thereby preventing surface damage. In this study, a

similar condition was observed. Manganese in the bulk material appears to play a comparable role in causing pits on the friction surface, particularly under PME grease conditions (see Fig. 11(f)). Tungsten particles in Petro grease specimen can restore the surface smoothness, even in cases of high wear (see Fig. 6). On the other hand, under PME-C grease condition, cellulose particles fill the pits on the contact interface, protecting the surface from severe friction and wear.

The most significant finding of this research is the formation of an aluminum oxide layer on the friction surface (see Fig. 9(e-f)). This layer appears to protect the surface from excessive friction and wear. In a previous study, it was reported that aluminum, along with carbon, was present at the contact interface of a tribo-pair lubricated with SAE 40 lubricants mixed with CNC additives [17]. However, that research utilized an aluminum plate as the friction material, meaning that the aluminum detected on the friction surface originated from the bulk material. In this study, the source of aluminum is uncertain, as it is not listed among the components of AISI 52100. Nevertheless, since aluminum has been detected by EDX on the friction surface of the tribo-pair lubricated with PME grease and PME-C grease, it is reasonable to conclude that the material used in this study likely contains a small amount of aluminum, despite its absence from the material composition list.

This research has demonstrated that CNC particles can be effectively utilized as an additive in grease lubricants. This is particularly true in the semi-solid state, where cellulose particles can be more uniformly dispersed within the lubricant compared to the liquid state. However, the effectiveness of cellulose particles can still be influenced by several factors, including particle concentration, temperature, type of grease thickener, and friction material. Furthermore, the effects of rheology have not been considered in this study. Therefore, additional research is essential to gain a deeper understanding of how those parameters influence friction and wear. This knowledge will ultimately contribute to the development of environmentally friendly lubricants derived from renewable materials.

3.5 Extreme pressure (EP) properties

An extreme pressure (EP) test was performed to ascertain the last non-seizure load and weld point of grease subjected to defined conditions. During the test, upon reaching the initial seizure condition, the lubricating film thickness decreased, resulting in significant adhesive wear between the contacting surfaces. With the increase in applied load, there was a significant rise in the friction between the contacting surfaces. As a result, the lubricating film was entirely compromised, leading to plastic deformation, which caused the surfaces of the ball material to adhere and become welded. Table 3 presents the final non-seizure loads documented for the formulated palm bio-greases.

Table 3. The EP properties.

Grease	Weld load (kg)
Palm Methyl Ester (PME)	150
Palm Methyl Ester with Cellulose (PME-C)	120

The results demonstrated that there was no significant change in the load-carrying capacity of the palm bio-greases, which were able to sustain the tribo-film until failure and seizing took place at 150 kg for PME and 120 kg for PME-C. The tribo-film in this instance was primarily derived from the base oil, with polar molecules present in the palm ester, including the carboxyl group of fatty acids, creating a thin lubricant layer that separates the contacting surfaces [42].

4. CONCLUSION

In summary, the friction tests conducted using a pin-on-disk reciprocating tribometer reveal improvements in the friction and wear characteristics of self-mated AISI 52100 tribo-pairs when lubricated with palm methyl ester (PME) grease containing cellulose nanocrystal (CNC) particles. The analysis of wear scars confirms that the performance of PME grease mixed with cellulose particles is comparable to that of commercial grease containing tungsten additives. Furthermore, the addition of cellulose particles to PME grease demonstrates enhanced friction and wear behavior compared to PME grease without the additive. The sliding tests were performed at an initial contact pressure of 1.039 GPa, utilizing a mixture of 1 mg of CNC in 100 ml of PME as the base lubricant.

The scanning electron microscopy (SEM) analysis of the surface morphology of the wear scar on the contact interface lubricated with PME grease containing CNC particles reveals a significantly smoother and flatter surface compared to that lubricated with PME grease without the additive. Energy-dispersive X-ray (EDX) analysis indicates the presence of oxygen and aluminum elements on the contact interface when PME grease contains CNC particles. It appears that a tribofilm composed of an aluminum oxide layer forms on the contact interface, which is responsible for protecting the contact area from severe friction and wear.

These results indicate that CNC particles can be used more effectively as additives in grease compared to their use in liquid lubricants. This is because CNC particles can be more stably dispersed in a semi-solid state than in a liquid state.

Acknowledgement

Funded by Universitas Syiah Kuala under Research Grant Ref. No: 169/UN11.2.1/ PG.01.03/SPK/PTNBH/2024.

REFERENCES

[1] Ganefri, R. Fadillah, and H. Hidayat, "Designing Interface Based on Digipreneur to Increase Entrepreneurial Interest in Engineering Students," *International Journal on Advanced Science Engineering and Information Technology*, vol. 12, no. 1, pp. 78–84, Jan. 2022, doi: 10.18517/ijaseit.12.1.13915.

[2] A. R. Bhat, R. Kumar, and P. K. S. Mural, "Natural fiber reinforced polymer composites: A comprehensive review of Tribo-Mechanical properties," *Tribology International,* vol. 189, p. 108978, Sep. 2023, doi: 10.1016/j.triboint.2023.108978.

[3] D. Rahmadiawan, N. Aslfattahi, N. Nasruddin, R. Saidur, A. Arifutzzaman, and H. A. Mohammed, "MXene Based Palm Oil Methyl Ester as an Effective Heat Transfer Fluid," *Journal of Nano Research,* vol. 68, pp. 17–34, Jun. 2021, doi: 10.4028/www.scientific.net/JNanoR.68.17.

[4] R. Shah, M. Woydt, and S. Zhang, "The economic and environmental significance of sustainable lubricants," *Lubricants*, vol. 9, no. 2, p. 21, Feb. 2021, doi: 10.3390/lubricants9020021.

[5] O. V. Săpunaru, A. E. Sterpu, C. A. Vodounon, S. Osman, and C. I. Koncsag, "Rheology of new lubricating greases made from renewable materials," *Analele Universităţii "Ovidius" Constanţa. Seria Chimie/"Ovidius" University Annals of Chemistry,* vol. 34, no. 2, pp. 91–98, Jul. 2023, doi: 10.2478/auoc-2023-0012.

[6] W. T. C. Fan, "*Regeneration of used petroleum-based lubricants and biolubricants by a novel green and sustainable technology*," Ph.D. dissertation, Dept. of Environmental Engineering, Univ. of Southern California, Los Angeles, CA, USA, 2010.

[7] D. Gasni, D. Rahmadiawan, R. Irwansyah, and A. E. Khalid, "Composite of Carboxymethyl Cellulose/MXene and SpAn 60 as additives to enhance tribological properties of Bio-Lubricants," *Lubricants*, vol. 12, no. 3, p. 78, Mar. 2024, doi: 10.3390/lubricants12030078.

[8] R. Kurniawan, Z. Fuadi, D. Rahmadiawan, M. A. Kalam, and A. Maulinda, "Improving Sliding Wear of AISI52100 Using Cellulose Microparticles Additive," *Materials Science Forum,* vol. 1150, pp. 75–82, Jun. 2025, doi: 10.4028/p-ym6zxC.

[9] N. Grishkewich, N. Mohammed, J. Tang, and K. C. Tam, "Recent advances in the application of cellulose nanocrystals," *Current Opinion in Colloid & Interface Science,* vol. 29, pp. 32–45, Feb. 2017, doi: 10.1016/j.cocis.2017.01.005.

[10] S.-C. Shi, S.-W. Ouyang, and D. Rahmadiawan, "Erythrosine–Dialdehyde cellulose nanocrystal coatings for antibacterial paper packaging," *Polymers*, vol. 16, no. 7, p. 960, Apr. 2024, doi: 10.3390/polym16070960.

[11] S.-C. Shi, S.-T. Cheng, and D. Rahmadiawan, "Developing biomimetic PVA/PAA hydrogels with cellulose nanocrystals inspired by tree frog structures for superior wearable sensor functionality," *Sensors and Actuators a Physical,* vol. 379, p. 115981, Oct. 2024, doi: 10.1016/j.sna.2024.115981.

[12] D. Rahmadiawan *et al.*, "Enhanced properties of TEMPO-oxidized bacterial cellulose films via eco-friendly non-pressurized hot water vapor treatment for sustainable and smart food packaging," *RSC Advances,* vol. 14, no. 40, pp. 29624–29635, Jan. 2024, doi: 10.1039/d4ra06099g.

[13] D. Rahmadiawan *et al.*, "A Novel Highly Conductive, Transparent, and Strong Pure-Cellulose Film from TEMPO-Oxidized Bacterial Cellulose by Increasing Sonication Power," *Polymers*, vol. 15, no. 3, p. 643, Jan. 2023, doi: 10.3390/polym15030643.

[14] R. K. Singh, O. P. Sharma, and A. K. Singh, "Evaluation of cellulose laurate esters for application as green biolubricant additives," *Industrial & Engineering Chemistry Research,* vol. 53, no. 25, pp. 10276–10284, May 2014, doi: 10.1021/ie501093j.

[15] K. Li *et al.*, "Friction reduction and viscosity modification of cellulose nanocrystals as biolubricant additives in polyalphaolefin oil," *Carbohydrate Polymers,* vol. 220, pp. 228–235, May 2019, doi: 10.1016/j.carbpol.2019.05.072.

[16] S. Thomas, S. Gopi, J. Jacob, J. Haponiuk, and G. Peter, "Use of Ginger Nanofibers for the Preparation of Cellulose Nanocomposites and Their Antimicrobial Activities," *Fibers*, vol. 6, no. 4, p. 79, Oct. 2018, doi: 10.3390/fib6040079.

[17] N. W. Awang, D. Ramasamy, K. Kadirgama, G. Najafi, and N. A. Che Sidik, "Study on friction and wear of Cellulose Nanocrystal (CNC) nanoparticle as lubricating additive in engine oil," *International Journal of Heat and Mass Transfer,* vol. 131, pp. 1196–1204, Dec. 2018, doi: 10.1016/j.ijheatmasstransfer.2018.11.128.

[18] M. Gulzar *et al.*, "Dispersion Stability and Tribological Characteristics of TiO2/SiO2 Nanocomposite-Enriched Biobased Lubricant," *Tribology Transactions,* vol. 60, no. 4, pp. 670–680, Jun. 2016, doi: 10.1080/10402004.2016.1202366.

[19] C. Sun, "True density of microcrystalline cellulose," *Journal of Pharmaceutical Sciences,* vol. 94, no. 10, pp. 2132–2134, Aug. 2005, doi: 10.1002/jps.20459.

[20] M. Kalin, J. Kogovšek, and M. Remškar, "Mechanisms and improvements in the friction and wear behavior using MoS 2 nanotubes as potential oil additives," *Wear*, vol. 280–281, pp. 36–45, Jan. 2012, doi: 10.1016/j.wear.2012.01.011.

[21] Z. Fuadi, D. Rahmadiawan, R. Kurniawan, F. Mulana, and H. Abral, "Effect of Graphene Nanoplatelets on Tribological Properties of Bacterial Cellulose / Polyolester Oil," *Frontiers in Mechanical Engineering,* vol. 8, pp. 1-11, Mar. 2022, doi: 10.3389/fmech.2022.810847.

[22] A. M. Borrero-lópez, C. Valencia, A. Blánquez, M. Hernández, M. E. Eugenio, and J. M. Franco, "Cellulose pulp- and castor oil-based polyurethanes for lubricating applications: Influence of streptomyces action on barley and wheat straws," *Polymers*, vol. 12, no. 12, pp. 2822, Nov. 2020, doi: 10.3390/polym12122822.

[23] M. Adamu, A. S. Abdullahi Bilal, and A. Mashi, "Production and Characterization of Biodegradable Grease from Neem Seed Oil," *Journal of Scientific and Engineering Research*, vol. 3, no. 3, pp. 39-42, 2016.

[24] A. E. Sterpu, G. Prodan, N. Teodorescu, I. M. Prodea, A. I. Dumitru, and C. I. Koncsag, "Lubricating greases from olive oil, corn oil and palm oil," *Revista de Chimie*, vol. 67, no. 8, pp. 1575-1582, Aug. 2016.

[25] A. Saxena, D. Kumar, N. Tandon, T. Kaur, and N. Singh, "Development of Vegetable Oil-Based Greases for Extreme Pressure Applications: An Integration of Non-toxic, Eco-Friendly Ingredients for Enhanced Performance," *Tribology Letters,* vol. 70, no. 4, Sep. 2022, doi: 10.1007/s11249-022-01651-x.

[26] N. Duy Anh, N. H. Van, and T. Van Hien, "Study on synthesis of biodegradable polyurea grease using modified vegetable oil," *Journal of Military Science and Technology,* no. FEE, pp. 279–284, Dec. 2022, doi: 10.54939/1859-1043.j.mst.fee.2022.279-284.

[27] C. Wu, S. Li, Y. Chen, L. Yao, X. Li, and J. Ni, "Tribological properties of chemical composite and physical mixture of ZnO and SiO2 nanoparticles as grease additives," *Applied Surface Science,* vol. 612, p. 155932, Dec. 2022, doi: 10.1016/j.apsusc.2022.155932.

[28] T.-T. Huang, D. Rahmadiawan, and S.-C. Shi, "Synthesis and characterization of porous silica and composite films for enhanced CO_2 adsorption: A circular economy approach," *Journal of Materials Research and Technology,* vol. 32, pp. 1460–1468, Aug. 2024, doi: 10.1016/j.jmrt.2024.08.003.

[29] X. Liang and H. Ji, "Tribological Properties of Lubricating Grease Additives Made of Silica and Silicon Carbide Nanomaterials," *Integrated Ferroelectrics,* vol. 225, no. 1, pp. 212–224, May 2022, doi: 10.1080/10584587.2021.1911243.

[30] C. Yan, Q. Zeng, Y. Hao, Y. Xu, and M. Zhou, "Friction-Induced Hardening Behaviors and Tribological Properties of 60NiTi Alloy Lubricated by Lithium Grease Containing Nano-BN and MoS2," *Tribology Transactions,* vol. 62, no. 5, pp. 812–820, May 2019, doi: 10.1080/10402004.2019.1619889.

[31] S. O. Ilyin, S. N. Gorbacheva, and A. Y. Yadykova, "Rheology and tribology of nanocellulose-based biodegradable greases: Wear and friction protection mechanisms of cellulose microfibrils," *Tribology International,* vol. 178, p. 108080, Nov. 2022, doi: 10.1016/j.triboint.2022.108080.

[32] R. Fachri, S. Rizal, S. Huzni, I. Ikramullah, and S. Aprilia, "Production of Cellulose Nanocrystal (CNC) Combine with Silane Treatment from Pennisetum Purpureum via Acid Hydrolysis," in *Lecture notes in mechanical engineering*, pp. 535–543, 2024, doi: 10.1007/978-981-99-7495-5_51.

[33] Z. Fuadi, M. Faisal, M. Dirhamsyah, M. Tadjuddin, and R. Kurniawan, "Tribological properties of self-mated SUS304 lubricated by palm methyl ester mixed lubricant at boundary lubrication," in *IOP Conference Series: Materials Science and Engineering*, vol. 796, no. 1, p. 012011, Mar. 2020, doi: 10.1088/1757-899X/796/1/012011.

[34] D. Klemm *et al.*, "Nanocellulose as a natural source for groundbreaking applications in materials science: Today's state," *Mater. Today*, vol. 21, no. 7, pp. 720–748, Apr. 2018, doi: 10.1016/j.mattod.2018.02.001.

[35] L. M. Kneissl, G. Gonçalves, R. Joffe, M. Kalin, and N. Emami, "Mechanical properties and tribological performance of polyoxymethylene/short cellulose fiber composites," *Polymer Testing,* vol. 128, p. 108234, Oct. 2023, doi: 10.1016/j.polymertesting.2023.108234.

[36] S. C. Shi, C. F. Lin, C. F. Liu, and T. H. Chen, "Tribological and mechanical properties of cellulose/PMMA composite," *Polymers and Polymer Composites,* vol. 30, Jan. 2022, doi: 10.1177/09673911221140935.

[37] C. Goralka *et al.*, "Friction and Wear Reduction of Tungsten Carbide and Titanium Alloy Contacts via Graphene Nanolubricant," *Lubricants*, vol. 10, no. 10, p. 272, Oct. 2022, doi: 10.3390/lubricants10100272.

[38] H. A. Zaharin, M. J. Ghazali, N. Thachnatharen, F. Ezzah, R. Walvekar, and M. Khalid, "Progress in 2D materials based Nanolubricants: A review," *FlatChem*, vol. 38, p. 100485, Feb. 2023, doi: 10.1016/j.flatc.2023.100485.

[39] J. Srivastava, T. Nandi, and R. K. Trivedi, "Experimental Investigations on Thermophysical, Tribological and Rheological Properties of MoS2 and WS2 Based Nanolubricants with Castor Oil as Base Lubricant," *Tribology in Industry,* vol. 45, no. 4, pp. 591–603, Dec. 2023, doi: 10.24874/ti.1472.04.23.07.

[40] Y. Zhang *et al.*, "Tribological properties of nano cellulose fatty acid esters as ecofriendly and effective lubricant additives," *Cellulose*, vol. 25, no. 5, pp. 3091–3103, Apr. 2018, doi: 10.1007/s10570-018-1780-9.

[41] Z. Fuadi, K. Adachi, and T. Muhammad, "Formation of Carbon-Based Tribofilm Under Palm Methyl Ester," *Tribology Letters,* vol. 66, no. 3, Jun. 2018, doi: 10.1007/s11249-018-1036-8.

[42] R. Zahid *et al.*, "Investigation of the tribochemical interactions of a tungsten-doped diamond-like carbon coating (W-DLC) with formulated palm trimethylolpropane ester (TMP) and polyalphaolefin (PAO)," *RSC Advances,* vol. 7, no. 43, pp. 26513–26531, Jan. 2017, doi: 10.1039/c6ra27743h.